Cross relaxation from the $^4G_{5/2}$ state of Sm^{3+} in $Cs_2NaSm_xY_{1-x}Cl_6$ and $Cs_2NaSm_xGd_{1-x}Cl_6$: a comparison of multipole-multipole and anisotropic dielectric shell models

1995 J. Phys.: Condens. Matter 7 9683

(http://iopscience.iop.org/0953-8984/7/49/029)

J. Phys.: Condens. Matter 7 (1995) 9683–9692. Printed in the UK

Cross relaxation from the $^4G_{5/2}$ state of Sm^{3+} in $Cs_2NaSm_xY_{1-x}Cl_6$ and $Cs_2NaSm_xGd_{1-x}Cl_6$: a comparison of multipole–multipole and anisotropic dielectric shell models

Thomas Luxbacher†, Harald P Fritzer† and Colin D Flint‡

† Institut für Physikalische und Theoretische Chemie, Technische Universität Graz, 8010 Graz, Austria

‡ Laser Laboratory, Department of Chemistry, Birkbeck College, 29 Gordon Square, London WC1H 0PP, UK

Received 15 June 1995

Abstract. Luminescence decay curves from the $^4G_{5/2}$ state of Sm^{3+} in cubic hexachloroelpasolite crystals $Cs_2NaSm_xY_{1-x}Cl_6$ and $Cs_2NaSm_xGd_{1-x}Cl_6$ ($x = 0.001$ to $x = 1$) have been measured in the temperature range 10–300 K. Energy transfer from the $^4G_{5/2}$ to the ^6F_J states occurs at all concentrations studied and is interpreted in terms of a discrete shell model. The transfer constant to a single acceptor in the first shell, k^{ET}, is much greater than the intrinsic decay constant of the isolated donor at all temperatures. We demonstrate that it is impossible to distinguish between a model involving an anisotropic local dielectric with dipole–dipole coupling and higher-order multipole–multipole coupling on the basis of measuring decay curves.

1. Introduction

The radiative and non-radiative energy transfer process involving lanthanide ions in inorganic solids are of considerable technological and scientific interest. The use of lanthanide ions in luminescent materials for display devices, lasers and upconverter phosphors has stimulated intensive studies of their properties in various crystalline environments. In most cases these investigations were made on lanthanides in non-centrosymmetric environments where the electric dipole no-phonon transitions within the $4f^N$ configuration are allowed [1].

For several years we have been interested in the energy levels and energy transfer processes in the cubic hexachloroelpasolites $Cs_2NsLnCl_6$ (Ln = rare-earth ion) [2–4]. In these systems the rare-earth ion occupies a perfect octahedral site, surrounded by six chloride ions. The electronic spectra are dominated by magnetic-dipole-allowed pure electronic origins and electric-dipole-allowed vibronic origins. The three odd-parity vibrations of the $[LnCl_6]^{3-}$ ion ($\bar{\nu}_3$, ν_4 and ν_6) appear strongly in the vibronic sidebands and are accompanied by weaker lattice vibrations. For several reasons these high-symmetry crystals are attractive model systems for the study of energy migration and transfer processes. Firstly, the transition dipoles associated with the f → f transitions at octahedral sites are relatively small and therefore the excited states of lanthanides in centrosymmetric complexes have long relaxation times. This offers possibilities for optical pumping, energy storage and energy transfer. Secondly, the ^SL_J levels are split into the minimum number of components

0953-8984/95/499683+10$19.50

for a crystalline solid so that the number of possible energy transfer pathways is minimized. Thirdly, the vibrational dispersion makes the vibronic sidebands much broader than the electronic origins in systems like, e.g., LaF_3, so that the energy transfer is not critically dependent on small changes in the exact positions of the electronic states involved.

It has become conventional to treat energy transfer within the Inokuti–Hirayama (IH) approximation [5]. However, as recognised by many authors [4, 6, 7], this model, which assumes a continuous distribution of acceptors surrounding the donor, is inapplicable to crystalline solids. The failure of the IH model is particularly severe at short donor–acceptor distances in high-symmetry crystals but short donor–acceptor distances dominate the energy transfer processes. Attempts, therefore, to determine whether the energy transfer mechanism is due to dipole–dipole, dipole–quadrupole, quadrupole–quadrupole or exchange interactions by 'fitting' experimental curves are likely to be misleading.

In this contribution we consider the relaxation of the $^4G_{5/2}$ excited state of Sm^{3+} in $Cs_2NaSm_xY_{1-x}Cl_6$ and $Cs_2NaSm_xGd_{1-x}Cl_6$ ($x = 0.001, \ldots, 1$). For large x and especially at high temperatures the emission from the $^4G_{5/2}$ state is strongly quenched due to cross relaxation involving the ^6F_J levels. We interpret the results in terms of a recently developed discrete shell model [8] and compare analyses using a variety of assumptions concerning the energy transfer process. A significant conclusion is that even when extensive, precise experimental data are available, unambiguous distinction between coupling mechanisms is not possible by 'fitting' the experimental data to theoretical models, even when the gross approximations of the IH method are removed.

2. The structural and spectroscopic properties of $Cs_2NaSmCl_6$

$Cs_2NaSmCl_6$ crystallizes in the $Fm3m$–O_h^5 space group at room temperature where the Sm^{3+} ion is on a perfect octahedral site surrounded by six chloride ions. The cubic lattice parameter a_0 is 10.8341(9) Å. The lattice parameter for Cs_2NaYCl_6 is 10.7315(15) Å, reflecting the smaller size of the Y^{3+} ion [9]. The lattice parameter of $Cs_2NaGdCl_6$, $a_0 = 10.7918(8)$, is much closer to that of $Cs_2NaSmCl_6$. Below 100 K the pure compound undergoes a phase transition to the $I4/m$–C_{4h}^5 space group which causes splittings of the degenerate electronic and vibronic energy levels in the order of a few wavenumbers. The diluted materials $Cs_2NaSm_xY_{1-x}Cl_6$ and $Cs_2NaSm_xGd_{1-x}Cl_6$ ($x \leqslant 0.5$) do not undergo a phase transition.

The electronic energy levels of $Cs_2NaSmCl_6$ are rather well established both theoretically and experimentally [10, 11]. The electronic transitions are dominated by magnetic-dipole-allowed electronic origins and electric-dipole-allowed vibronic origins. In octahedral symmetry the $^6H_{5/2}$ ground state is split into two crystal field components, Γ_7 (0 cm^{-1}) and Γ_8 (178 cm^{-1}). The luminescent electronic state $^4G_{5/2}$ is also split into two components, Γ_8 (17 760 cm^{-1}) and Γ_7 (18 105 cm^{-1}). The vibrational properties of $Cs_2NaSmCl_6$, Cs_2NaYCl_6 and $Cs_2NaGdCl_6$ are also well established [10]. The odd-parity vibrational modes of the $[SmCl_6]^{3-}$ ion are about 80 cm^{-1} (ν_6), 100 cm^{-1} (ν_4) and 250 cm^{-1} (ν_3). Lattice vibrations are at 40 and 180 cm^{-1}.

A rather large number of cross relaxation processes involving $^4G_{5/2}$ to ^6F_J ($J = 5/2, 7/2, 9/2, 11/2$) relaxation at the donor and $^6H_{5/2}$ to ^6F_J ($J = 5/2, 7/2, 9/2, 11/2$) transitions at the acceptor might be involved in the quenching of the luminescence of the pure compound. Some of these are illustrated in figure 1. In principle these processes may occur by electric-dipole-vibronic–electric-dipole-vibronic (EDV–EDV) or magnetic dipole–magnetic dipole (MD–MD) mechanisms or involve higher electric multipoles. The possibility of a superexchange mechanism cannot be excluded *a priori*.

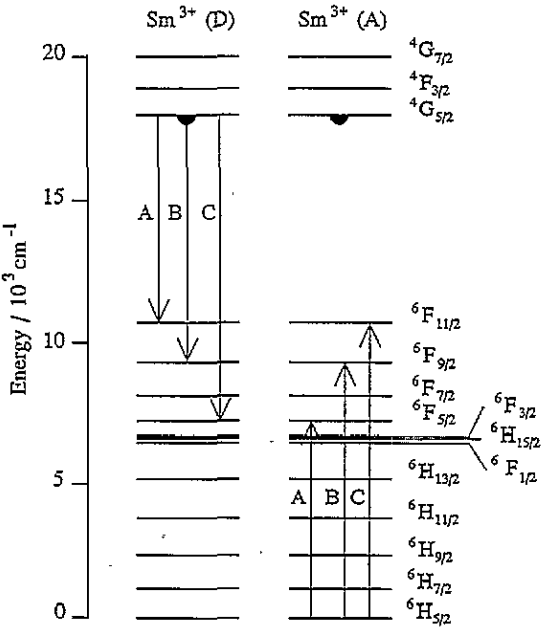

Figure 1. A selection of possible energy transfer pathways in Sm^{3+}.

3. Experimental details

Single crystals of $Cs_2NaSm_xY_{1-x}Cl_6$ and $Cs_2NaSm_xGd_{1-x}Cl_6$ were grown by the Bridgman technique as previously described [12]. Whilst both systems gave large, well formed crystalline products, the optical quality of the Gd samples was noticeably higher than that of the Y samples.

Luminescence decay observed at 16500±20 cm^{-1} was measured over a temperature range of 10 K to 300 K for the excitation into the $^4G_{5/2}(\Gamma_8)$ level at 17760 cm^{-1} as previously described [12].

4. The shell model for cross relaxation

The elpasolite structure is schematically shown in figure 2 and the positions of the ions of shells 1–4 and 6 are indicated. It is clearly impossible to describe the energy transfer processes using a model (such as that proposed by Inokuti and Hirayama) which assumes that the distribution of acceptors increases monotonically as the square of the donor–acceptor distance.

Our shell model assumes Förster–Dexter multipole–multipole interactions [13, 14] between statistically distributed donor and acceptor ions and within this model the luminescence decay curves following a δ-function excitation pulse take the form

$$I(t) = I(0)\exp(-k_0 t)\prod_{n=1}^{shells}\sum_{r_n=0}^{N_n} O_{r_n}^{N_n}(x)\exp\left[-r_n G_n^p\left(\frac{R_1}{R_n}\right)^{s_p} k^{ET} t\right]. \qquad (1)$$

The model assumes that excitation intensities are low, that there is no back transfer and that migration amongst the donors is negligible. x is the mole fraction of the rare-earth ion, R_n is the distance between the donor ion and an acceptor ion in the nth shell, k_0 is the radiative decay rate and k^{ET} is the energy transfer rate to a single acceptor in the first

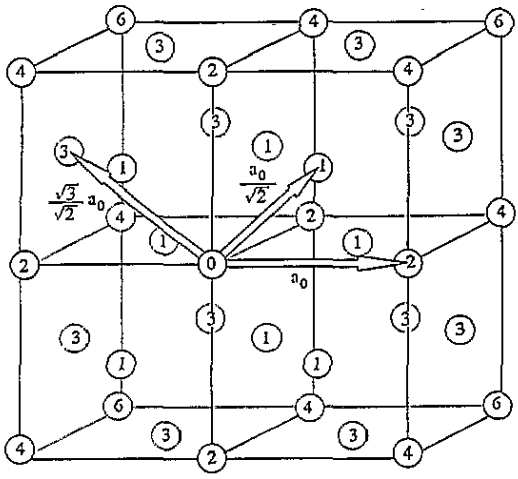

Figure 2. Part of the crystal lattice of elpasolites showing the distances to the three nearest neighbours.

shell. $s_p = 6$, 8 or 10 for EDV–EDV, EDV–EQ and EQ–EQ interactions, respectively. For $s_p = 6$ the angular dependence, G_n^6, of the coupling is independent of the value of n [8] and is included in the definition of k^{ET}. For higher multipole–multipole couplings this geometric factor changes from shell to shell. These geometric factors have been calculated and will be published elsewhere, but we shall show that their inclusion within the model is not justified for the experimental data presented in this paper.

The occupancy factor $O_{r_n}^{N_n}(x)$ is the statistical probability of there being exactly r_n acceptor ions in the nth shell which has a capacity to contain N_n acceptors and is readily computed from the equation

$$O_{r_n}^{N_n}(x) = \frac{N_n!}{(N_n - r_n)!r_n!}x^{r_n}(1-x)^{N_n - r_n}. \tag{2}$$

For the elpasolite lattice, more than 94% of the energy transfer processes are described by using the first three shells. In this preliminary study we truncate the expansion at this point. All values of the occupancy factor have been included. This represents a summation over 2275 acceptor distributions. There is a further assumption within any tractable energy transfer model that the microscopic dielectric constant contains no angular or radial dependence terms. This is clearly impossible and raises the question of how to deal with the radial dependence of the medium permittivity within shell models. We consider experimental aspects of this problem later in this paper.

5. Results

The excitation and absorption spectra corresponding to the $^6H_{5/2} \rightarrow {}^4G_{5/2}$ transition have been reported elsewhere [10, 11].

Figure 3 shows the luminescence decay of the $^4G_{5/2}(\Gamma_8) \rightarrow {}^6H_{7/2}(\Gamma_8, \Gamma_7)$ transitions of $Cs_2NaSm_{0.001}Gd_{0.999}Cl_6$ and of the pure Sm compound at 10 K. Note that the time axes differ by a factor of 256. Both decay curves are accurately exponential over more than ten lifetimes. The decay constant for $x = 0.001$ is 58 s^{-1} and represents the decay rate of an isolated Sm^{3+} ion in the $Cs_2NaGdCl_6$ lattice at 10 K. Within the three-shell model, the decay constant for the pure material can be shown to be $k_0 + (12 + 6/8 + 24/27 + \ldots) \times k^{ET} \approx k_0 + 13.64 \times k^{ET}$ for dipole–dipole interactions and $k_0 + (12 + 6/32 + 24/243 + \ldots) \times k^{ET} \approx k_0 + 12.29 \times k^{ET}$ for quadrupole–quadrupole

interactions [8]. The measured exponential decay constant for $x = 1$ at 10 K is 11 600 s^{-1} corresponding to $k^{ET}(DD) = 850\ s^{-1}$ and $k^{ET}(QQ) = 940\ s^{-1}$, respectively. At higher temperatures the decay curves remain exponential with the energy transfer rate increasing by a factor of 2.7 at 300 K. The derived values of k_0, $k^{ET}(DD)$ and $k^{ET}(QQ)$ are given in table 1. For $0.02 \leqslant x \leqslant 0.5$ the decay curves exhibit an initial faster, non-exponential decay, the proportion of the faster process increasing with increasing x (figure 4).

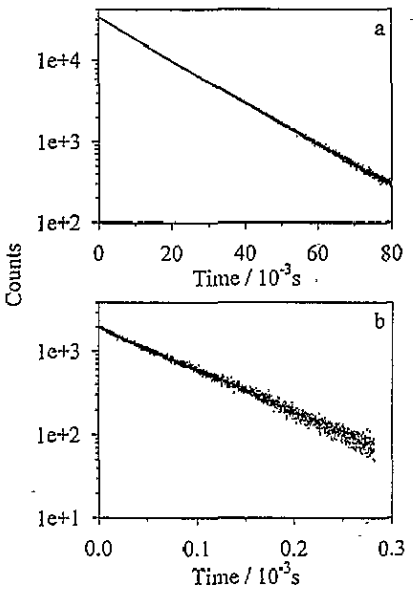

Figure 3. Luminescent decay curves for very dilute (a) and pure crystals (b) at 10 K. Note that the time scale differs by a factor of 256.

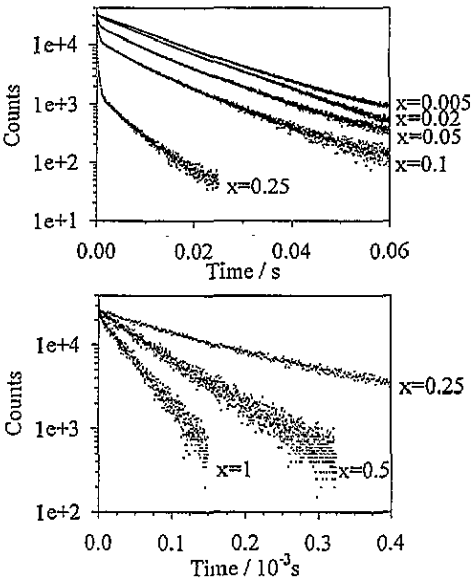

Figure 4. Luminescent decay curves of the $^4G_{5/2} \rightarrow {}^6F_J + {}^6H_J$ in $Cs_2NaSm_xY_{1-x}Cl_6$ emission as a function of x.

Table 1. Kinetic data for the relaxation of the $^4G_{5/2}$ state of $Cs_2NaSm_xGd_{1-x}Cl_6$ as a function of temperature.

T (K)	k_0 (s^{-1})†	$k^{ET}(DD)$ (s^{-1})‡	$k^{ET}(QQ)$ (s^{-1})‡
10	58	840	940
20	58	910	1010
40	61	1100	1220
60	65	1230	1370
80	66	1350	1490
100	71	1480	1650
140	77	1670	1860
170	83	1830	2030
300	107	2270	2520

† Experimental decay rates for $x = 0.001$.

‡ Energy transfer rates to a single acceptor in the first shell calculated from experimental values for $x = 1$.

Figure 5 shows the temperature dependence of the decay curves for $x = 0.25$. At all temperatures the decay curves again consist of an initial non-exponential fast process

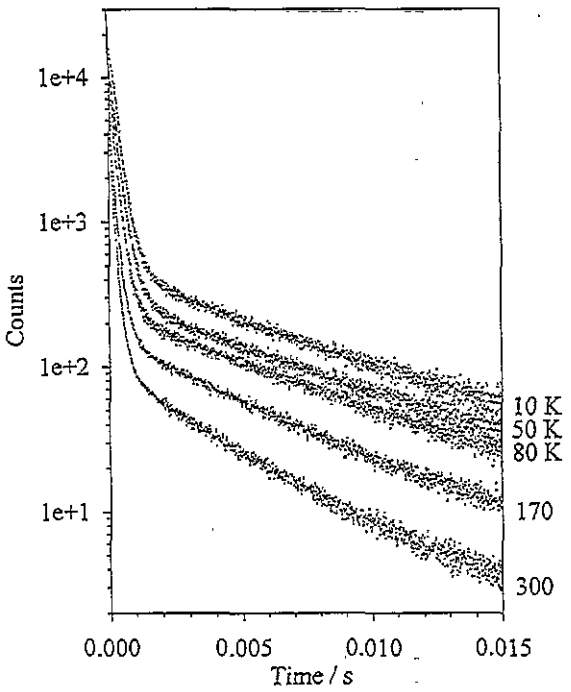

Figure 5. The time dependence of the $^4G_{5/2}$ emission of $Cs_2NaSm_{0.25}Gd_{0.75}Cl_6$ as a function of temperature.

followed by a slightly non-exponential slower region. The proportion of the fast process increases with increasing temperature. The temperature dependence of k_0 is consistent with a normal vibronic intensity mechanism following the coth law with a mean vibrational frequency comparable to that of ν_3. The temperature dependence of k^{ET} is slightly stronger. This is as expected since transitions involving ν_6 and ν_4 as well as ν_3 contribute to the energy transfer mechanism. Since k^{ET} is about 15 times greater than k_0 almost all of the information concerning energy transfer is contained within the first 3×10^{-3} of the decay curves. Thereafter for $x < 1$ the curves are asymptotic to the decay of the isolated ion although this is only experimentally realizable for $x \leqslant 0.25$. Figure 6 shows the comparison of the early part of the experimental decay curve for $x = 0.25$ at 175 K with the calculated decay curve (e) for dipole–dipole coupling using the values of k_0 and k^{ET}(DD) from table 1. It is clear that the model fails to describe the data except at very short times. A similar problem occurs for all temperatures and all intermediate concentrations and for both the Y and Gd crystals.

Somewhat better agreement could be obtained by artificially reducing the contributions from the second and third shells compared to the first. This could be taken to indicate that the energy transfer process is of shorter range than is given by the dipole–dipole mechanism. Curves b and d are the corresponding calculated curves assuming EDV–EQ and EQ–EQ interactions. Essentially, perfect agreement was obtained using values of s somewhat greater than ten. This might be interpreted as indicating that the cross relaxation involved a very high-order multipole–multipole coupling.

There is a more plausible explanation of the discrepancy between the experimental results and the calculated curve for dipole–dipole coupling, that acceptors in the second and third shells are selectively screened from the donor. Examination of the model of the elpasolite structure or of figure 1 in [8] shows that the coupling between the donor and a nearest-neighbour acceptor occurs through regions of relatively low electronic density,

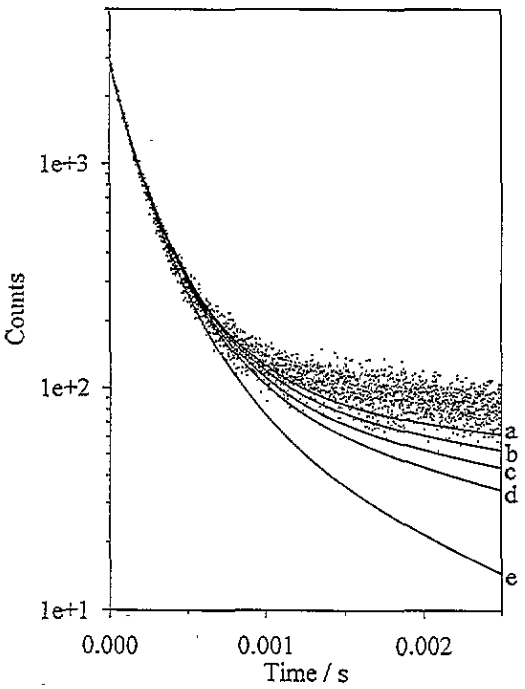

Figure 6. A comparison between calculated decay curves assuming EDV–EDV (e), EDV–EQ (d) and EQ–EQ (b) mechanisms as well as EDV–EDV with screening of the second and third shells (0.1 and 0.3 for curves a and c, respectively) with experimental data for $x = 0.25$ at 175 K.

whereas coupling between the donor and an acceptor in the $n = 2$ shell involves the presence of two intervening chloride ions and one sodium ion. It is likely that the high charge density along the direction of this interaction would lead to a screening of the multipole–multipole coupling. A similar, but somewhat smaller, screening would also occur between the donor and $n = 3$ acceptor. The energy transfer therefore needs to be modified to include the detailed surroundings of the donor ion. Curves a and c in figure 6 show the effects of introducing screening factors of 0.1 and 0.3, respectively. Note that these curves are of very similar shape to curve b where we assumed an EQ–EQ mechanism. At a value of the screening factor immediate to that assumed in curves a and c, the calculated curve is indistinguishable from curve b. A distinction between the explanations involving higher-order multipoles and selective screening cannot be made on the basis of experimental decay curves.

A third process, the existence of a superexchange pathway via the intervening chloride ions and cations, exists in principle. This mechanism for energy transfer to the $n = 1$ shell requires a pathway through at least two chloride ions. Energy transfer to shells with $n > 1$ requires the involvement of further anions or cations. These latter processes are surely negligible. Whilst superexchange to the $n = 1$ shell also seems unlikely, we note that the decay kinetics do not permit a distinction between this and any other mechanism involving solely the $n = 1$ shell.

Other considerations might be responsible for our difficulties in modelling the experimental data. One possibility is energy migration in the $^4G_{5/2}$ level. For this process to be significant within the first 2×10^{-3} s, the energy migration rate must be fast as compared

with the energy transfer rate. The $^4G_{5/2} \leftrightarrow {}^6H_{5/2}$ transition is magnetic dipole allowed. Whilst migration by an MD–MD mechanism is feasible, the inhomogeneous broadening effects considered above will substantially reduce the rate of such a progress. Migration would lead to the experimental decay rate being faster than the calculated rate and the long-time decay rates would not be asymptotic to the decay of the isolated ion which is again not observed even at times $>10^{-2}$ s. There is no evidence for a change in the mechanisms occurring in this compound over the whole concentration and temperature ranges studied. This would appear to exclude migration as a significant contributor to the decay kinetics.

A second explanation is that the local concentration of acceptors around a donor is substantially lower than that calculated from stoichiometry. To model the decay curves on this assumption requires very large local deviations from the bulk concentration. Such an affect might be attributed to the difference in ionic radii of the host lattice and the Sm^{3+} ion. Since we obtain essentially identical results for both the Y and the appreciably larger Gd matrix (figure 7), this effect appears to be negligible. We now consider the likelihood of the first two processes in greater detail.

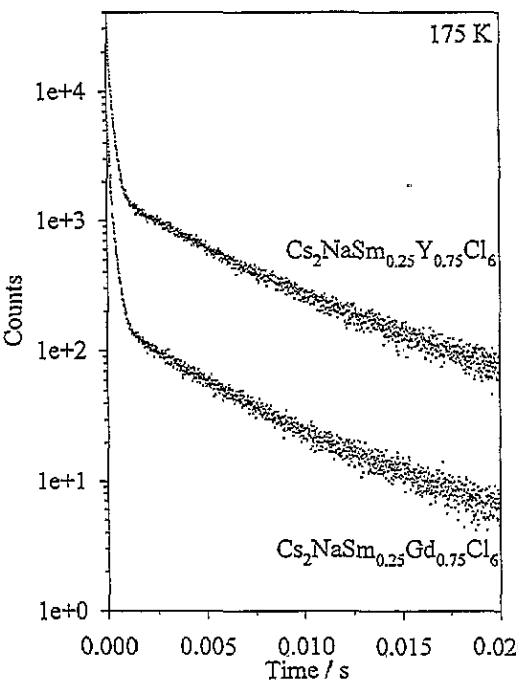

Figure 7. An example of the identity of decay curves for the Y and Gd hosts.

5.1. Higher-order multipole processes

In the elpasolite lattice the dominant energy transfer process occurs to the first shell. But, as above, if only this shell is considered there is no *experimental distinction between* dipole–dipole processes and higher-order multipolar processes. Such distinction can only be achieved by consideration of further shells which make only a minor contribution to the energy transfer process. For dipole–dipole processes the contributions from second and third shells are approximately equal. As the assumed order of the coupling process is increased the contribution from the outer shells falls off more rapidly. Essentially perfect agreement between the calculated and experimental curves can be achieved for all

concentrations and all temperatures using a value of s slightly greater than ten. Moreover the k^{ET} values obtained were comparable to those given in table 1. This could be interpreted as indicating that the energy transfer process proceeds by the EQ–EQ mechanism. Banerjee and Schwartz [10, 15] have claimed to observe the pure electric quadrupole transition Γ_7 ($^6H_{5/2}$) $\rightarrow$ $\Gamma_6(^6F_{1/2})$ in $Cs_2NaSmYCl_6$. This transition is calculated to be unusually strong for a quadrupole transition of a lanthanide ion [16] but is not involved in our cross relaxation process. An examination of all possible pairs of quadrupolar transitions at the donor and acceptor transitions in the absence of vibronic and vibrational contributions to the transition moment identifies only the $(^4G_{5/2})\Gamma_8 \rightarrow b\Gamma_8(^7F_{11/2})$ donor transition and the $(^6H_{5/2})\Gamma_7 \rightarrow \Gamma_8(^6F_{5/2})$ acceptor transition or alternatively the $(^4G_{5/2})\Gamma_8 \rightarrow \Gamma_8(^6F_{5/2})$ donor transition and the $(^6H_{5/2})\Gamma_7 \rightarrow a\Gamma_7(^6F_{11/2})$ acceptor transition as having significant spectral overlap within experimental error. The contribution of the EQ–EQ coupling to the energy transfer process for these transitions is calculated to be much smaller than that of the EDV–EDV process at distances of 7 Å and greater. Therefore EQ–EQ cross relaxation process seems unlikely in comparison with the EDV–EDV mechanism. Whilst vibrational dispersion will ensure that the EDV–EDV mechanism will not be sensitive to very small spectral shifts, almost all of the tiny quadrupole moments of the transitions involved in the cross relaxation will be localized at the electronic origin. At very low temperatures we might expect these origins to have homogeneous linewidths of less than 1 cm^{-1}; fortuitous spectral overlap is therefore unlikely. Moreover, inhomogeneous broadening of these lines by the electric fields created by substitution of Y^{3+} for Sm^{3+} would be expected to reduce the quadrupolar–quadrupolar coupling substantially [17]. Even if we suppose that fortuitous overlap of the quadrupolar transitions occurs in the presence of inhomogeneous broadening, it would be reasonable to suppose that this overlap would change as homogeneous broadening becomes important at higher temperatures. This would lead to a change in the mechanism as the temperature is increased. Figure 5 gives no evidence for such a change. This broadening is likely to occur by a two-phonon Raman process which leads to a T^7 dependence of the linewidths at modest temperatures [18]. The overlap of two such homogeneously broadened transitions would then be expected to have a very strong temperature dependence but we have shown that the temperature dependence of k^{ET} is only slightly faster than that of k_0 and is in any case consistent with the coth law.

Many of the objections raised above for the EQ–EQ mechanism do not apply to the EDV–EQ mechanism. Curve d in figure 6 shows that this mechanism does not describe the data well.

5.2. Non-isotropic dielectric dipole–dipole coupling

There are a large number of possible vibronic transitions involving $^4G_{5/2}$ to ^6F_J levels at the donor and $^6H_{5/2}$ to ^6F_J levels at the acceptor where there is substantial spectral overlap. A satisfactory description of the experimental data within the EDV–EDV transfer mechanism requires the assumption of a process which reduces the role of second- and third-neighbour spheres of acceptors. The effects of the screening of donor and acceptor coupling by intervening anions and cations might be modelled by the assumption of an effective non-spherical dielectric about the donor.

There seems no quantitative way of estimating the effects of this non-uniform dielectric without an explicit calculation, which would not be easy. The experimental data can be modelled rather well within the EDV–EDV approximation by assuming a screening factor of 0.1 for both the second and third shells. There is, of course, no reason to expect that the screening factors for both of these shells should be equal. We note that reduction factors

of four for shell $n = 2$ and nine for $n = 3$ produce a decay equation which is numerically identical to the quadrupolar–quadrupolar mechanism considered above. Whilst it would be possible to determine a mean value of the shielding factor or even individual values of the shielding factors of shells two and three by 'curve fitting' the experimental data, such values are likely to be meaningless except for in summarizing the experimental data.

Therefore, in spite of the large number of high-quality data available to us, the small contribution to the total decay kinetics from the second and third shells makes the experimental distinction between the inhomogeneous dielectric model and the assumption of the importance of higher-order multipoles impossible by the examination of decay curves. As described above, we regard the higher-order multipole interaction as extremely unlikely in this case. We note that the assumption of an inhomogeneous dielectric may also be made within the EDV–EQ or EQ–EQ mechanisms.

6. Conclusions

The shell model of energy transfer shows the impossibility of distinguishing from experimental data between higher-order multipole coupling, inhomogeneous dielectric and superexchange models for energy transfer in the lanthanide elpasolites. The time dependence of the decay processes predicted by an EQ–EQ mechanism (or processes involving higher-order multipoles) and the inhomogeneous dielectric model are experimentally indistinguishable especially if simultaneous EDV–EDV, EDV–EQ and EQ–EQ mechanisms are present. Any such distinction must depend on theoretical calculations of the observed rate constants. It seems most likely that EDV–EDV and/or EDV–EQ coupling are the primary energy transfer mechanisms in these materials but both require the assumption that the energy transfer is not isotropic in this cubic compound.

Acknowledgment

This work has been supported in part under the collaborative ARC scheme of the British Council and the Bundesministerium für Wissenschaft und Forschung.

References

[1] Nakazawa E and Shionoya S 1967 *J. Chem. Phys.* **47** 3211 and references 1–19 therein
[2] Bettinelli M and Flint C D 1990 *J. Phys.: Condens. Matter* **2** 8417
[3] Bettinelli M and Flint C D 1991 *J. Phys.: Condens. Matter* **3** 4433
[4] Bettinelli M and Flint C D 1991 *J. Phys.: Condens. Matter* **3** 7053
[5] Inokuti M and Hirayama F 1965 *J. Chem. Phys.* **43** 1978
[6] Dornauf H and Heber J 1980 *J. Lumin.* **22** 1
[7] Huber D L 1979 *Phys. Rev.* B **20** 2307
[8] Vasquez S O and Flint C D 1995 *Chem. Phys. Lett.* **238** 379
[9] Morss L R, Siegal M, Stenger L and Edelstein N 1970 *Inorg. Chem.* **9** 1771
[10] Banerjee A K and Schwartz R W 1981 *Chem. Phys.* **58** 255
[11] Foster D R, Richardson F S and Schwartz R W 1985 *J. Chem. Phys.* **82** 618
[12] Luxbacher T, Fritzer H P, Sabry-Grant R and Flint C D *Chem. Phys. Lett.* **241** 103
[13] Förster T 1948 *Ann. Phys., Lpz.* **2** 55
[14] Dexter D L 1953 *J. Chem. Phys.* **21** 836
[15] Schwartz R W and Banerjee A K 1981 *Chem. Phys. Lett.* **79** 19
[16] Tanner P A and Siu G G 1992 *Mol. Phys.* **75** 233
[17] Luxbacher T, Fritzer H P and Flint C D 1995 *Chem. Phys. Lett.* **233** 571
[18] McCumber D E and Sturge M D 1963 *J. Appl. Phys.* **34** 1682